



A theoretical study on the electronic and optical properties of M-TiO₂/ZnO (M=Li, Na, K, Fe) toward application in photocatalysis

Nguyen Thi Kim Giang¹, Nguyen Thu Hien¹, Duong Quoc Hoan¹ and Nguyen Thi Thu Ha^{1,*}

¹Hanoi National University of Education, 136 Xuan Thuy, Cau Giay, Hanoi, Vietnam;

*Email: ntt.ha@hnue.edu.vn

ARTICLE INFO

Received: 18/3/2024

Accepted: 25/5/2024

Published: 30/6/2024

Keywords:

TiO₂-ZnO composite, metal dopant, photocatalyst

ABSTRACT

This study employs the tight-binding density functional method GFN1-xTB to investigate the structural and electronic properties of TiO₂-ZnO and TiO₂-ZnO composite materials modified by Li, Na, K, and Fe metals. Computational analyses reveal the formation of weak covalent bonds between the TiO₂ and ZnO components within the composite system. Doping TiO₂-ZnO with metals induces significant alterations in the electronic structure, particularly in terms of ionization energy and global electrophilic index. The UV-VIS spectra are calculated using real-time time-dependent density functional theory with xTB Hamiltonians. The obtained results demonstrate minimal impact of metal presence on the absorption spectrum of TiO₂-ZnO, but significant influence on the recombination potential of photogenerated charge carriers. It is suggested that Fe/TiO₂-ZnO and Li/TiO₂-ZnO will demonstrate higher photocatalytic activity than the pristine TiO₂-ZnO material.

1. Introduction

Photocatalysis has emerged as an advanced technology in the field of environmental remediation and energy production. Among the various photocatalysts, titanium dioxide (TiO₂) and zinc oxide (ZnO) have received substantial attention owing to their remarkable properties. The integration of nano materials has enabled the development of flexible and highly efficient catalysts. The combination of TiO₂ and ZnO presents a unique synergistic effect that capitalizes on the individual advantages of each material. When combined, ZnO facilitates the efficient transfer of photogenerated electrons to the surface of TiO₂, minimizing charge recombination and prolonging the lifetime of charge carriers [1]. Furthermore, the TiO₂-ZnO structure has an increased surface area and an abundance of reaction sites. This high surface area provides more sites for adsorption of target pollutants

[1,2]. From a different perspective, the enhancement of photocatalytic activity in semiconductors, such as TiO₂ and ZnO, may be achieved by including trace elements such as metal doping. Experimental investigations have illustrated that the introduction of metal doping alters the bandgap of the system, consequently impacting the behavior of charge carriers and leading to a reduction in recombination rates [3,4]. Moreover, the characteristics of TiO₂ or ZnO semiconductors are considerably influenced not only by the incorporation of transition metals but also by the presence of alkali metals as dopants [5,6]. For instance, the introduction of lithium doping into TiO₂ beads achieves the improvement of electronic properties through the reduction of electronic trap states [6]. In the research conducted by Giahi et al. [7], it was demonstrated that 10 mol% Fe-doped ZnO-TiO₂ exhibited the highest photocatalytic efficiency in the degradation of linear alkylbenzene sulfonate. However, the authors did not

<https://doi.org/10.62239/jca.2024.035>

identify the underlying cause or clarify the role of Fe. Similarly, doping Li onto TiO₂ also demonstrated a significant influence on the material's optical properties. Ravishankar et al. [8] highlighted the beneficial effect of lithium on the photocatalytic activity of TiO₂ in trypan blue degradation, attributing it to lithium's ability to trap electrons and its reduction on the surface of TiO₂.

Despite numerous experimental studies that have demonstrated the effective photocatalytic activity of the TiO₂-ZnO composite system, as well as the potential performance enhancement through metal doping, there is still a limited number of theoretical researches exploring the impact of metal doping on the structure and properties of TiO₂-ZnO composite materials. It is also important to emphasize that the interaction between the doped metal atoms and the TiO₂-ZnO structure, as well as their influence on the electronic properties of the material, has not been clearly elucidated. Therefore, this study aims to present a theoretical research finding concerning the electronic and optical properties of metal-doped TiO₂-ZnO (M/TiO₂-ZnO) composite materials, where M = Li, Na, K and Fe. The computational results will offer valuable insights at the molecular level into the interactions among the components in the composite systems, as well as shed light on the role of metal atoms in enhancing the photocatalytic activity. Consequently, this will provide valuable guidance for researching and designing novel catalytic material systems based on TiO₂-ZnO composites.

2. Experimental

The model of the TiO₂-ZnO system was established using the (101) anatase TiO₂ surface structure with a lattice size of 3×3×2, alongside a (ZnO)₆ cluster. The rationale for choosing the (ZnO)₆ cluster is based on its stability in a three-dimensional structure, since it represents the smallest stable 3D ZnO cluster. The TiO₂-ZnO model was built by placing the cluster on the TiO₂ surface.

The metallic elements chosen for doping into the TiO₂-ZnO system represent alkali metals (Li, Na, K), and a transition metal – Fe. In the M/TiO₂-ZnO model, a solitary metal atom is selected for introduction into the TiO₂-ZnO system by replacing with one Zn atom in the cluster (ZnO)₆.

All optimization calculations and energy evaluations were carried out using the Tight-Binding Quantum

Chemical Method named GFN1-xTB which is integrated in the DFTB+ software [9]. The GFN1-xTB approach is parametrized to cover all spd-block elements and lanthanides up to atomic number 86, using reference data at the hybrid density functional theory level.

To figure out the electronic properties of the studied M/TiO₂-ZnO systems, the Mulliken atomic charges (q), the vertical ionization potential (IP), vertical electron affinity (EA), global electrophilic index (GEI) were calculated and analyzed.

The UV-Vis spectrum of the material are investigated using real-time time-dependent density functional theory (RT-TD-DFT) with the xTB Hamiltonians operator.

3. Results and discussion

Figure 1 illustrate the optimized structures of TiO₂-ZnO and M/TiO₂-ZnO.

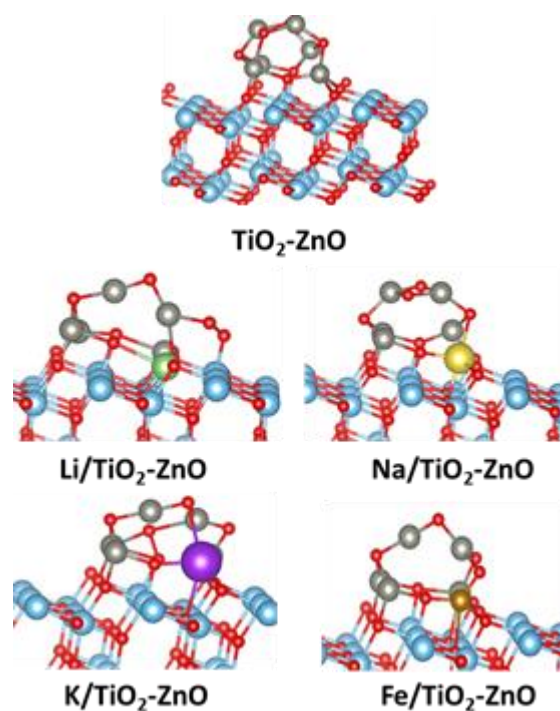


Fig 1: Optimized structures of M/TiO₂-ZnO

The obtained results indicate that the bond length values of Ti – O in the TiO₂-ZnO optimized structure are 1.929 Å and 1.973 Å, which exhibit good agreement with the experimental findings. The deposition of ZnO onto the surface of TiO₂ results in the formation of chemical bonds between the Zn atoms of ZnO and the O atoms on the TiO₂ surface, characterized by bond orders of 0.624 and 0.590. Additionally, bonds are produced between the Ti atoms of TiO₂ and the O

atoms of ZnO, with bond orders of 1.032 and 0.94. However, the ZnO cluster retains its geometric structure, whereas the geometric properties of TiO₂ remain substantially unaltered. Therefore, the TiO₂/ZnO system can be categorized as a composite material. This classification arises from the presence of weak covalent bonds between the TiO₂ and ZnO components, which allows for the maintenance of their distinct two-phase structures.

The calculated bond orders (Table 1) indicate that the Fe atom has the capacity to form multiple chemical bonds with O atoms in both ZnO and TiO₂. In contrast, alkaline atoms possess only one valence electron, which is significantly lower than that of Fe. As a result, they tend to form bonds with a single O atom. Moreover, it's important to note that the Fe atom demonstrates the ability to establish donor bonds, resulting in stronger interactions between Fe and O compared to alkali metals.

Table 1: Bond orders (BO) formed between M atom and O atoms of TiO₂-ZnO and atomic charge (q) on metal atom

M	Fe	Li	Na	K
BO(M-O(TiO ₂))	0,716	0,203	<0,06	<0,06
BO(M-O(ZnO))	2,127; 1,215	<0,06	0,136	0,159
q(M), e	+ 0,193	+ 0,810	+ 0,920	+ 0,623

The alkali metal atoms carry a considerably higher positive charge compared to that observed on the Fe atom. This phenomenon can be explained by the differences in electronegativity values and atomic radius between alkali metals and iron, leading to alkali metals having a higher tendency to lose electrons compared to Fe. Indeed, the electronegativity values for Li, Na, K, and Fe are 0.98, 0.93, 0.82 and 1.83, while their atomic radii are 152 pm, 186 pm, 232 pm and 126 pm, respectively [10]. Among the alkali metals, it is observed that the charge changes in the following order: K < Li < Na. The non-monotonic variation of the Mulliken charge values across alkali metal atoms has not been clearly explained in the literature. One possible reason, in our view, could be the significant difference in atomic radii between K and Zn (232 pm and 134 pm, respectively), so the substitution of Zn with K affects the polarization induced by the O²⁻

anions. Additionally, the bond order between metals and oxygen shows an increasing trend in the following sequence: Na < K < Li. The estimated bond order exclusively considers covalent bonds and does not consider additional interactions, such as electrostatic interactions. Table 2 presents the results of calculating IP (eV), EA (eV) and GEI (eV) for the studied systems.

Table 2: Calculated IP, EA and GEI

M	-	Fe	Li	Na	K
IP	8,886	8,887	8,733	8,683	8,634
EA	7,070	7,027	6,930	6,924	6,870
GEI	17,51	17,23	17,012	17,31	17,04

The obtained results indicate that the introduction of Fe dopant leads to a slight increase in the IP. Conversely, the presence of alkali metals in the system causes a reduction in the IP. The most significant reduction in IP is observed in the case of K. The impact of the introduced metallic elements on the system's EA is relatively small compared to the influence of ionization potential, since EA measures the system's capacity to accept electrons, and all introduced elements are metals.

The GEI index, which quantifies the surface acidity of a material, indicates that the inclusion of metals in the TiO₂-ZnO system leads to a reduction in acidity. This observation aligns perfectly with the outcomes obtained from the computation of the atomic charges, wherein all metal atoms exhibit a positive charge.

The results of UV-Vis spectrum (Figure 2) analysis for TiO₂-ZnO and M/TiO₂-ZnO (M = Fe, Na, Li, K) reveal that the introduction of metal atoms into the material system hardly alters its shape or the position of maximum adsorption in the UV-Vis spectrum compared to the original material. Given that the TiO₂-ZnO system comprises hundreds of atoms, incorporating just one metal atom yields negligible effects on the optical properties of the material system.

It is important to emphasize that the enhancement of photocatalytic activity in TiO₂-ZnO based materials primarily aims to reduce the recombination of photogenerated electrons and holes. While certain theoretical calculation methods, such as Marcus theory, have been employed to investigate electron transfer rates, they are not without limitations [11]. In a previous publication by our group [12], we introduced the idea of assessing the recombination of photogenerated electrons and holes based on the electron density

distribution in the reduction and oxidation regions, as well as the spatial separation between these regions. Additionally, the impact of the spatial distance between HOMOs and LUMOs on the optical properties of materials has also been addressed in various other studies [13]. In this study, in order to assess the potential for recombination between electrons and photogenerated holes, it is assumed that electrons transition from the conduction band (HOMO) to the valence band (LUMO), resulting in holes in the HOMO and photogenerated electrons in the LUMO. We proceed to calculate the spatial distance (d_{H-L}) between the position with the highest electron density on the HOMO and the LUMO. The calculation results can be found in Table 3.

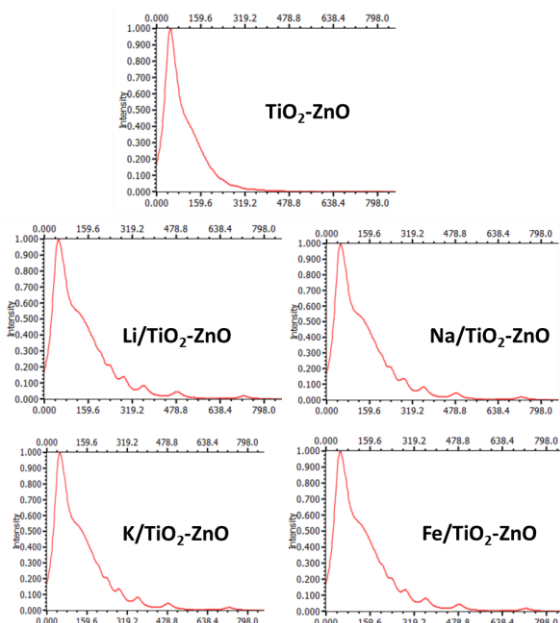


Figure 2: Calculated UV-spectrum of TiO_2/ZnO and $\text{M}/\text{TiO}_2\text{-ZnO}$

Table 3: Spatial distance between HOMO and LUMO of the systems

M	-	Fe	Li	Na	K
d_{H-L} , Å	6,09	7,65	9,28	6,10	2,93

It is observed that doping $\text{TiO}_2\text{-ZnO}$ with Fe and Li leads to an increase in d_{H-L} values, while the presence of Na has no effect. However, the introduction of K results in a reduction of the d_{H-L} . Under the assumption that a greater distance between the HOMO and LUMO implies a lower ability of recombination between photogenerated electrons and holes, it can be predicted that the inclusion of Fe and Li in the $\text{TiO}_2\text{-ZnO}$ composite will diminish the potential for recombination between photogenerated electrons and holes, consequently enhancing the catalytic activity of

the material. These findings completely consistent with the results of HOMO and LUMO image analysis of the material systems (Figure 3).

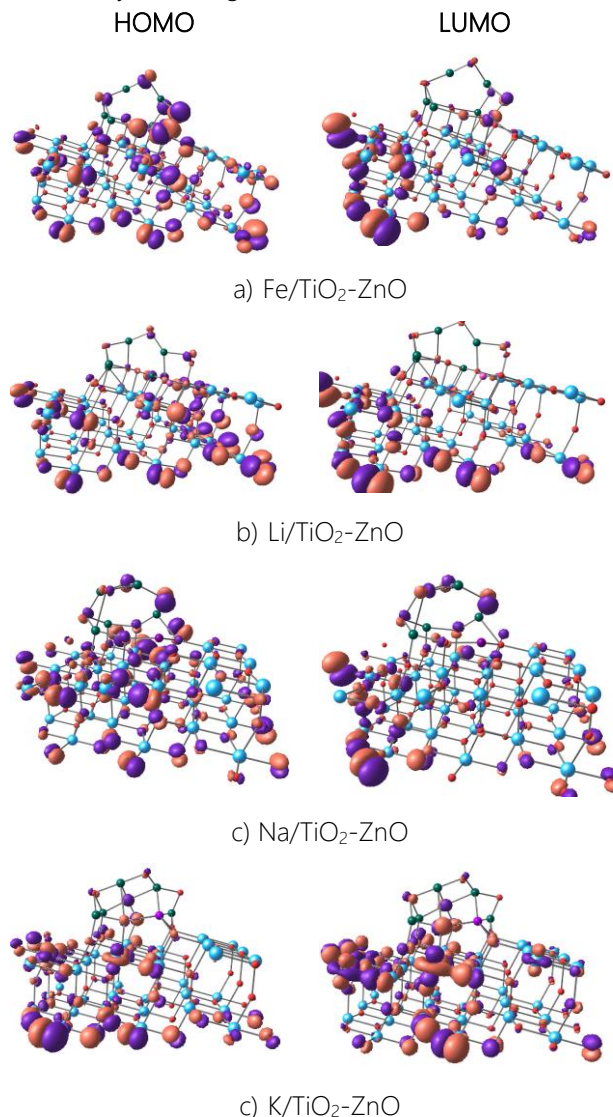


Figure 3: HOMO and LUMO of $\text{Fe}/\text{TiO}_2\text{-ZnO}$ (a), $\text{Li}/\text{TiO}_2\text{-ZnO}$ (b), and $\text{K}/\text{TiO}_2\text{-ZnO}$ (c) depicted at an isovalue of $0.03 \text{ eV}/\text{Å}$

In the Li, Na, $\text{K}/\text{TiO}_2\text{-ZnO}$ systems, alkali metals, with only one valence electron, are mainly involved in bonding processes with oxygen atoms. Analysis of the HOMO and LUMO images of these systems indicates that alkali metal atoms make minimal contributions to either the HOMO or LUMO of the system. However, it is important to note that in the cases of $\text{Li}/\text{TiO}_2\text{-ZnO}$, the HOMO and LUMO distributions extend to opposite sides, whereas for Na and K, these frontier orbitals are distributed on the same side. Meanwhile, for $\text{Fe}/\text{TiO}_2\text{-ZnO}$, HOMO is primarily situated on the oxygen atoms, being evenly distributed throughout the system. On the other hand, LUMO is predominantly located on

one side of the oxygen atom in TiO_2 . The d atomic orbitals of the Fe atom contribute to both the HOMO and LUMO of the system. The spatial separation between the HOMO and LUMO in $\text{Fe/TiO}_2\text{-ZnO}$ and $\text{Li/TiO}_2\text{-ZnO}$ is significant. This is attributed to the high electron density on Fe and Li atoms. Fe possesses multiple valence electrons capable of engaging in optical processes, whereas Li has the smallest atomic radius among alkali metals.

This means that the spatial distance between reduced and oxidized regions, as well as between electrons and photogenerated holes, is extensive. This substantial separation effectively slows down the recombination process, ultimately enhancing the photocatalytic ability of semiconductors. The computational findings are entirely consistent with previously published experimental results regarding the impact of Fe and Li doping on ZnO-TiO_2 [7,8].

4. Conclusion

Using the GFN1-xTB tight-binding density functional method, the study examined the structural, electronic, and optical properties of $\text{TiO}_2\text{-ZnO}$, along with $\text{TiO}_2\text{-ZnO}$ materials modified by Li, Na, K, and Fe metals. The calculations revealed the formation of weak covalent bonds between the components TiO_2 and ZnO in the composite system. Doping $\text{TiO}_2\text{-ZnO}$ with metals resulted in alterations in the electronic structure of the material, particularly in terms of ionization energy and global electrophilic index. While the presence of the metal had minimal impact on the absorption spectrum of $\text{TiO}_2\text{-ZnO}$, it did affect the recombination potential of photogenerated electrons and holes. It is anticipated that the material systems $\text{Fe/TiO}_2\text{-ZnO}$ and $\text{Li/TiO}_2\text{-ZnO}$ will exhibit high photocatalytic activity.

Acknowledgments

This research is funded by Vietnam National Foundation for Science and Technology Development (NAFOSTED) under grant number 104.06–2020.48.

References

1. C. Cheng, A. Amini, C. Zhu, Z. Xu, H. Song, N. Wang, *Scientific Reports* 4(1) (2014) 4181. <https://doi.org/10.1038/srep04181>
2. D. Chen, H. Zhang, S. Hu, J. Li, *The Journal of Physical Chemistry C* 112(1) (2007) 117–122. <https://doi.org/10.1021/jp077236a>.
3. S. I. Mogal, V.G. Gandhi, M. Mishra, S. Tripathi, T. Shripathi, P. A. Joshi, D. O. Shah, *Industrial & Engineering Chemistry Research* 53(14) (2014) 5749–5758. <https://doi.org/10.1021/ie404230q>.
4. N.K. Pal, C. Kryschi, *Chemosphere* 144 (2016) 1655–1664. <https://doi.org/10.1016/j.chemosphere.2015.10.060>
5. C. Rajeevgandhi, S. Bharanidharan, T. Jayakumar, N. Shailaja, P. Anand, L. Gudanathan, C. Ashok Kumar, *Solid State Communications* 371 (2023) 115256. <https://doi.org/10.1016/j.ssc.2023.115256>.
6. P. Golvari, E. Nouri, N. Mohsenzadegan, M. R. Mohammadi, S. O. Martinez-Chapa, *New Journal of Chemistry* 45(5) (2021) 2470–2477. <https://doi.org/10.1039/D0NJ04051G>
7. M. Gahi, S. Saadat Niavol, H. Taghavi, M. Meskinfam, *Russian Journal of Physical Chemistry A* 89(13) (2015) 2432–2437. <https://doi.org/10.1134/s0036024415130154>
8. T.N. Ravishankar, G. Nagaraju, Jairton Dupont, *Materials Research Bulletin* 78 (2016) 103–111. <https://doi.org/10.1016/j.materresbull.2016.02.017>
9. DFTB+ <https://dftbplus.org/>.
10. J. Speight, *Lange's Handbook of Chemistry*, Seventeenth Edition; McGraw Hill Professional, 2016.
11. Z. Shuai, W. Li, J. Ren, Y. Jiang, H. Geng, *The Journal of Chemical Physics* 153(8) (2020) 080902 <https://doi.org/10.1063/5.0018312>
12. N. T. T. Ha, P. T. Be, P. T. Lan, N. T. Mo, L. M. Cam, N. N. Ha, *RSC Advances* 11(27) (2021) 16351–16358. <https://doi.org/10.1039/d1ra01237a>
13. S. V. Badalov, R. Wilhelm, W. G. Schmidt, *Journal of Computational Chemistry* 41 (2020) 1921–1930. <https://doi.org/10.1002/jcc.26363>